

Lecture Notes in Mechanical Engineering

Hemant B. Mehta
Manish K. Rathod
Rufat Abiev
Müslüm Arıcı *Editors*

Recent Advances in Thermal Sciences and Engineering


Select Proceedings of ICAFFTS 2021

 Springer

Lecture Notes in Mechanical Engineering


Series Editors

Fakher Chaari, National School of Engineers, University of Sfax, Sfax, Tunisia

Francesco Gherardini , Dipartimento di Ingegneria “Enzo Ferrari”, Università di Modena e Reggio Emilia, Modena, Italy

Vitalii Ivanov, Department of Manufacturing Engineering, Machines and Tools, Sumy State University, Sumy, Ukraine

Editorial Board

Francisco Cavas-Martínez , Departamento de Estructuras, Construcción y Expresión Gráfica Universidad Politécnica de Cartagena, Cartagena, Murcia, Spain

Francesca di Mare, Institute of Energy Technology, Ruhr-Universität Bochum, Bochum, Nordrhein-Westfalen, Germany

Mohamed Haddar, National School of Engineers of Sfax (ENIS), Sfax, Tunisia

Young W. Kwon, Department of Manufacturing Engineering and Aerospace Engineering, Graduate School of Engineering and Applied Science, Monterey, CA, USA

Justyna Trojanowska, Poznan University of Technology, Poznan, Poland

Lecture Notes in Mechanical Engineering (LNME) publishes the latest developments in Mechanical Engineering—quickly, informally and with high quality. Original research reported in proceedings and post-proceedings represents the core of LNME. Volumes published in LNME embrace all aspects, subfields and new challenges of mechanical engineering.

To submit a proposal or request further information, please contact the Springer Editor of your location: **Europe, USA, Africa:** Leontina Di Cecco at Leontina.dicecco@springer.com **China:** Ella Zhang at ella.zhang@springer.com **India:** Priya Vyas at priya.vyas@springer.com **Rest of Asia, Australia, New Zealand:** Swati Meherishi at swati.meherishi@springer.com Topics in the series include:

- Engineering Design
- Machinery and Machine Elements
- Mechanical Structures and Stress Analysis
- Automotive Engineering
- Engine Technology
- Aerospace Technology and Astronautics
- Nanotechnology and Microengineering
- Control, Robotics, Mechatronics
- MEMS
- Theoretical and Applied Mechanics
- Dynamical Systems, Control
- Fluid Mechanics
- Engineering Thermodynamics, Heat and Mass Transfer
- Manufacturing
- Precision Engineering, Instrumentation, Measurement
- Materials Engineering
- Tribology and Surface Technology

Indexed by SCOPUS and EI Compendex.

All books published in the series are submitted for consideration in Web of Science. To submit a proposal for a monograph, please check our Springer Tracts in Mechanical Engineering at <https://link.springer.com/bookseries/11693>

Hemant B. Mehta · Manish K. Rathod ·
Rufat Abiev · Müslüm Arıcı
Editors

Recent Advances in Thermal Sciences and Engineering

Select Proceedings of ICAFFTS 2021

 Springer

Editors

Hemant B. Mehta
Department of Mechanical Engineering
S. V. National Institute of Technology
Surat, India

Manish K. Rathod
Department of Mechanical Engineering
S. V. National Institute of Technology
Surat, India

Rufat Abiev
Department of Optimization of Chemical
and Biotechnological Equipment
Saint Petersburg State Institute
of Technology
Saint Petersburg, Russia

Müslüm Arıcı
Department of Mechanical Engineering
Kocaeli University
Kocaeli, Türkiye

ISSN 2195-4356

ISSN 2195-4364 (electronic)

Lecture Notes in Mechanical Engineering

ISBN 978-981-19-7213-3

ISBN 978-981-19-7214-0 (eBook)

<https://doi.org/10.1007/978-981-19-7214-0>

© The Editor(s) (if applicable) and The Author(s), under exclusive license to Springer Nature Singapore Pte Ltd. 2023

This work is subject to copyright. All rights are solely and exclusively licensed by the Publisher, whether the whole or part of the material is concerned, specifically the rights of translation, reprinting, reuse of illustrations, recitation, broadcasting, reproduction on microfilms or in any other physical way, and transmission or information storage and retrieval, electronic adaptation, computer software, or by similar or dissimilar methodology now known or hereafter developed.

The use of general descriptive names, registered names, trademarks, service marks, etc. in this publication does not imply, even in the absence of a specific statement, that such names are exempt from the relevant protective laws and regulations and therefore free for general use.

The publisher, the authors, and the editors are safe to assume that the advice and information in this book are believed to be true and accurate at the date of publication. Neither the publisher nor the authors or the editors give a warranty, expressed or implied, with respect to the material contained herein or for any errors or omissions that may have been made. The publisher remains neutral with regard to jurisdictional claims in published maps and institutional affiliations.

This Springer imprint is published by the registered company Springer Nature Singapore Pte Ltd. The registered company address is: 152 Beach Road, #21-01/04 Gateway East, Singapore 189721, Singapore

Contents

Experimental Investigation on Passive Direct Methanol Fuel Cell with Dissimilar Current Collector Materials	1
N. V. Raghavaiah and G. Naga Srinivasulu	
Performance Comparison of Different Geometries of Thermal Energy Storage Unit for Solar Cooker	15
B. C. Anilkumar, Ranjith Maniyeri, and S. Anish	
Automobile Air Conditioning Loads Modelling Using Heat Balance Method	27
Vanita Wagh and A. D. Parekh	
Computational Modelling of Bioheat Transfer for Hyperthermia Using Finite Difference Method	45
Tarun Hegde and Ranjith Maniyeri	
Application of Phase Change Material in Electronic Heat Dissipation: State-Of-The-Art	59
Kapil Kalra and Amit Arora	
Experimental Study of Integrated Solar Dryer with and Without Reversed Absorber and Reflector	71
Vijay R. Khawale, Bhojraj N. Kale, and Sandeep Lutade	
An Overview on Composites Used in Phase Change Materials for Battery Thermal Management System	87
Nishi Mehta, Shivam Prajapati, and Shulabh R. Yadav	
Effect of Semi-cylindrical Protrusions on Thermal Behaviour of SPHE	99
Darshilkumar N. Chhatrodiya, Kuldeep Parmar, Jay Chavda, Yash Kalola, and Vipul M. Patel	
Thermal Analysis for Solar Water Heater by Implementing Fins	113
Rushil Patel, Harshal Sonawane, Yogesh Mane, and Mandar Lele	

Emission Analysis Through Numerical Simulation of Three-Way Catalytic Converter with Thermal Energy Storage	125
Sanket S. Keer, Gargee Pise, and M. R. Nandgaonkar	
Optimization of 3D Plate Fin Heat Sinks Through Analytical Modelling	139
Niyaj Shikalgar, Pushkar Chitale, and S. N. Sapali	
Comparative Energy Analysis of R1234yf and R134a Refrigerants	151
Vanita Wagh and A. D. Parekh	
Recent Trends in Artificial Intelligence-Inspired Electronic Thermal management—A Review	165
Aviral Chharia, Nishi Mehta, Shivam Gupta, and Shivam Prajapati	
Investigation on Heat Transfer Performance of Nanofluids	177
Shankar Durgam and Ganesh Kadam	
A Comprehensive Review on Nano-additives for the Enrichment of Diesel and Biodiesel Blends for Engine Applications	187
Gandhi Pullagura, Srinivas Vadapalli, V. V. S. Prasad, Venkateswarlu Velisala, Kodanda Rama Rao Chebattina, and Abdul Razack Mohammad	
Convective-Radiative Heat Transfer in a Rotating Cubic Cavity with a Local Heat Source	207
S. A. Mikhailenko and M. A. Sheremet	
Performance Analysis of IC Engine Using Parabolic Fin	215
Ruchika Dnyaneshwar Lande, Onkar Pravinrao Ajegaonkar, Swapnil Suresh Nikam, Yogesh Mane, and Mandar M. Lele	
Numerical Study on Operating Temperature of PV and PV-PCM Systems	227
Deepak Kumar Sharma, Manish K. Rathod, and Purnanand V. Bhale	
Aluminum Oxide as Potential Additives to N-Butanol-Diesel Blends on Emission and Performance Characteristics of the Diesel Engine	241
Gandhi Pullagura, Srinivas Vadapalli, V. V. S. Prasad, Suryanarayana Varma Datla, Arhun Jaya Sai Makkena, Ashok Srinivas Reddy Chilla, Venkateswarlu Velisala, and Kodanda Rama Rao Chebattina	
Analytical Study of Thermal Stresses Generated in a Carbon Fiber-Reinforced Wheel Hub	257
Prasanna Kadambi, Bikash Prasad, Pranay Luniya, Parth Kulkarni, Sandip T. Chavan, and Yogesh G. Mane	

Estimation of Emissivity of the Surface Using Jaya Algorithm 265
 Sanil Shah and Ajit Kumar Parwani

Development of an Empirical Model for the Prediction of Thermoelectric Behavior of Lithium Iron Phosphate Pouch Cell Under Different Discharge Rates 273
 Indraneel Naik, Pravin Nemade, and Milankumar Nandgaonkar

Application of Artificial Neural Network to Predict Effective Thermal Conductivity of Porous Foam Structure 285
 Vipul M. Patel, Harsh Kumar, and Kuldeep Singh

Numerical Analysis of Heat Transfer Enhancement of Heat Sink Using Different Phase Changing Materials for Electronic Cooling Application 299
 K. Naga Ramesh, M. Manoj Sai, K. Vineeth Goud, K. Raghavendra, S. Amruth, and T. Karthikeya Sharma

Performance Analysis of Active Cooling System in Lithium-Ion Batteries Using Dual Potential Multi-Scale Multi-Dimensional Battery Model Approach in Extreme Environment 311
 Ashima Verma and Dibakar Rakshit

Numerical Investigation on Characteristics of Methane Combustion 321
 Keyur Kadia, Nikhil A. Baraiya, and R. D. Shah

Computational Heat Transfer Analysis of Perforated Annular Fin with Highly Conductive Insert Under Forced Convection 333
 S. Lakshmanan and M. Venkatesan

Membrane Electrode Assembly Material for DMFC-A Review 345
 Seema S. Munjewar, Arunendra K. Tiwari, and Rohan Pande

Thermal Management of Lithium-Ion Battery Pack with Liquid Cooling: A Computational Investigation 357
 Shankar Durgam and Vikrant Mahesh Deshmukh

Heat Transfer Characteristics of a Two-Phase Closed Vertical Thermosyphon: An Experimental Study 371
 Aalekh Srivastava, Manish K. Rathod, and Naresh Yarramsetty

Application of Inverse Heat Transfer Technique in Thin Slab Continuous Casting for Estimating the Interfacial Boundary Heat Flux 385
 Ananda S. Vaka, Pedduri Jayakrishna, Saurav Chakraborty, Suvankar Ganguly, and Prabal Talukdar

Heat Transfer Enhancement of Fin and Tube Heat Exchanger Using Ribs	399
Vaidant Rathore, Atharva A. Lokhande, Yogesh G. Mane, and Mandar M. Lele	
Effect of Dilution on Lean Blow-Off Limit of Methane Combustion	409
Keyur Kadia, Nikhil A. Baraiya, and R. D. Shah	
Experimental Investigation on the Performance of Solar Stills with Vent Holes and Hybrid Nano PCM	421
M. Padmanaban, S. Suresh, and P. Kalidoss	
Performance Characterization of Domestic Liquefied Petroleum Gas Cookstove	437
Kishan Dash and Sikata Samantaray	
Improvement in the Electric Vehicle Battery Performance Using Phase Change Material	447
Jay R. Patel and Manish K. Rathod	
Effect of Dilution on Emission from Methane Combustion	459
Keyur Kadia, Nikhil A. Baraiya, and R. D. Shah	
Energy and Exergetic Analysis of Thermal Transport in Latent Heat Thermal Energy Storage Systems Impregnated with Metal Foam	473
Varun Joshi, Jay R. Patel, and Manish K. Rathod	
Numerical Investigation on Finned Latent Heat Storage Unit	485
Nitish Gupta and Manish K. Rathod	
Material Recovery from End-of-Life Solar Photovoltaic Module Through Thermal and Chemical Processes	499
Aparna Singh, Ahmed Ali Kabir, Sachin Gupta, Jyotsna Singh, and R. B. Singh	
Effect Analysis of Heat Extraction on the Performance of the TAE	513
S. R. Solanki, A. B. Desai, and H. B. Mehta	

About the Editors

Dr. Hemant B. Mehta is currently an associate professor at the Department of Mechanical Engineering, National Institute of Technology Surat, Gujarat. He obtained his B.E. (Mechanical), M.Tech. (Turbomachines) and Ph.D. from the National Institute of Technology, Surat, Gujarat. His major areas of research interests include two-phase flow induced heat transfer in micro and minichannels, active and passive thermal management using microchannel heat sink, heat pipe and its variants and nanofluids, CFD analysis of thermal systems, radiative heat transfer and thermoacoustic engine/refrigerator. He has published more than 50 articles at national and international levels and he has been granted five design patents. He completed two research projects of Rs. 35 lakhs. He is a Fellow of Institution of Engineers and a life member of Indian Society of Heat and Mass Transfer.

Dr. Manish K. Rathod is currently an assistant professor at the Department of Mechanical Engineering, National Institute of Technology (SVNIT), Surat, India. He obtained his B.E. (Mechanical) and M.E. (Thermal Sciences) from M S University of Baroda and Ph.D. from SVNIT Surat. His area of interest is thermal energy storage using phase change material (PCM), Thermal management by PCM, Passive cooling in buildings, Energy and exergy analysis of thermal systems, Heat exchangers design and its augmentation. He has more than 70 journal/conference publications of the nation and international repute and 4 design patents in the field of his research. He was awarded Outstanding Scientist in Mechanical Engineering by the 4th Venus International Research Awards. He has published a book chapter entitled “Thermal Stability of Phase Change Material” in a book named Phase Change Materials and Their Applications.

Prof. Dr. Sc. Rufat Abiev is a Professor and Head in the Department of Optimization of Chemical and Biotechnological Equipment, Saint Petersburg State Institute of Technology (Technical University), Saint Petersburg, Russia. His research interest lies in Process Intensification, Microreactors, Process Simulation, Bubbles and Droplets break up, Heat- and Mass Transfer intensification, Pulsations for chemical engineering. Rufat Abiev has more than 450 publications, 6 books, 5 chapters

in a *New Handbook of Chemist and Technologist* (in Russian), 2 chapters in handbooks (*Process Analysis, Design, and Intensification in Microfluidics and Chemical Engineering*, Hershey, PA: IGI Global, USA, 2019; *Transport Processes at Fluidic Interfaces*, Springer-Verlag, Germany, 2017), more than 100 papers in peer-reviewed international and Russian journals and more than 90 patents. Several patents are implemented in the industry.

Prof. Müslüm Arıcı is a faculty member in Thermodynamics and Heat Technique Division of Mechanical Engineering Department of Kocaeli University, Turkey. He completed Diploma Course at von Karman Institute, Belgium in 2007. He received Ph.D. degree from Kocaeli University in 2010. He worked in Fluid Mechanics Research Group, University of Zaragoza, Spain in 2014 and 2016–2017 as a visiting professor. He has co-authored of more than 100 papers in refereed journal papers and presented numerous research papers in international conferences. He has been invited to as an invited speaker in several international conferences and workshops held in Croatia, Algeria, Ukraine, China, and Kazakhstan. He has served as a guest editor and has been in the editorial board of several international journals. His fields of interest are Numerical Heat Transfer, Computational Fluid Dynamics, Nanofluids, Solar Energy, Energy Efficient Buildings and Thermal Management by Phase Change Materials.

Experimental Investigation on Passive Direct Methanol Fuel Cell with Dissimilar Current Collector Materials



N. V. Raghavaiah and G. Naga Srinivasulu

Abstract Experimental investigation is carried out on passive direct methanol fuel cell, to study with the selected combination of different anode and cathode current collectors which have high electrical and thermal conductivity together with corrosion resistance compatibility properties. These collectors are fabricated with an opening ratio of 45.3% on Stainless Steel Grade-316L, Nickel-201 and brass (70% Cu-30% Zn) and experimented at 5 M concentration of methanol solution. Polarisation curves and maximum power density curves have been drawn with the experimental results for performance comparison using Ni-SS, Ni-Brass, SS-Ni and SS-brass anode and cathode combinations of current collectors. Comparative studies for maximum power and current densities are investigated and represented on bar charts for identifying the better combination of anode and cathode materials. Performance of cell is found best with the combination using Nickel-201 as anode and brass as cathode. With this combination, the maximum power density developed is 7.157 mW cm^{-2} , and the maximum current density produced is 65.6 mA cm^{-2} at 5 M concentration.

Keywords Passive direct methanol fuel cell · Current collector · Corrosion resistance material · Electrical conductivity · Thermal conductivity · Nickel · Stainless steel · Brass

Nomenclature

CC	Current collector
CD	Current density
MEA	Membrane electrode assembly
Ni	Nickel
PD	Power density

N. V. Raghavaiah (✉) · G. N. Srinivasulu
National Institute of Technology, Warangal, Telangana State, India
e-mail: nvraghavaiah@student.nitw.ac.in

PTFE	Polytetrafluoroethylene
pDMFC	Passive direct methanol fuel cell
SS	Stainless Steel

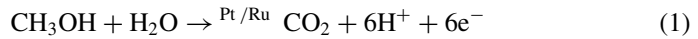
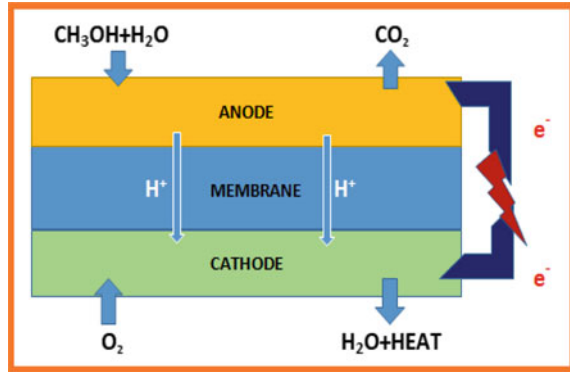
1 Introduction

With increase in societal demand for electricity every year across the globe, fuel cell technology is evolving out as one of the protuberant energy resources among the accessible alternative energy resources in place of fossil fuels which are going to be lost within next few decades. Fuel cells are similar to conversion devices like a battery; it converts the chemical energy of reactants into electricity leaving other reaction compounds as by-products [1]. However, fuel cell differs from a battery in that as long as the fuel and oxygen are supplied, it produces electric power continuously. Out of the other well-known fuel cells classified based on proton conducting membrane electrolyte, polymer exchange electrolyte membrane-based cell working with direct liquid feed methanol as fuel and air as an oxidant emerges out as an electric power source for the applications [2] of portable electronic appliances like mobile phones, laptops, tape recorders, Walkman, toys, computers, cell phones, emergency lights, including material handling equipment like forklifts, cargo loaders, etc., and also for space application systems [3]. As a fuel, liquid methanol is relatively inexpensive and easily available and has more specific energy density, quick refuelling and good transportation and better storage facility. Further, fuel cell characteristics are ultimately affected by significant aspects such as choice and make use of suitable materials and its novel designing. These fuel cells facilitate to operate at low temperatures and pressures without additional liquid electrolyte requirement [4]. pDMFC can also be operated at ambient pressure and temperatures conditions. It has other advantages like clean by-products, extremely no/low emission of oxides of nitrogen and sulphur, operates quietly, not having any moving parts and extra fuel processing to meet demand requirement and high energy. Compact cell design of pDMFC makes it easy to handle. Schematic representation of passive direct methanol fuel cell is represented in Fig. 1.

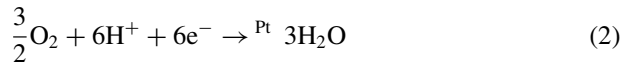
To have better reaction kinetics, pDMFC makes use of ruthenium and platinum as catalyst on the anodic side of the membrane to break the chemical bonds in the methane water solution to form carbon dioxide, hydrogen ions (protons) and free electrons as shown in Eq. (1). In the cell, the liberated electrons flow from the anodic side of the cell through an external circuit to the cathodic side, and the protons are transported through the proton conducting electrolyte membrane. At the cathode, the electrons and hydrogen ions react with oxidant to form water as shown in Eq. (2). The liberated heat of reaction is mostly released to surroundings through cathode side current collector. Overall chemical reaction of the cell is shown in Eq. (3).

Anode End Reaction:

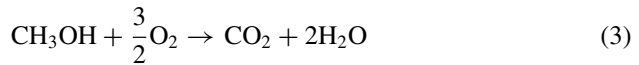
Fig. 1 Schematic representation of passive direct methanol fuel cell



Cathode End Reaction:



Overall Fuel Cell Reaction:



2 Literature Survey

Passive direct methanol fuel cell is getting importance across the globe as an electrical power source due to high-energy density of fuel. Among the fuel cell components, current collector material properties and their compatibility in water–methanol solution are influencing cell durability, performance and effectiveness.

Braz et al. [5] has studied the optimization process of passive direct methanol fuel cell with various current collector materials. It is indicated that to ascertain DMFC commercially, an optimum balance between its price, competence and durability should be achieved. Current collectors are accountable for about 70–80% of the system weight, and different current collector materials were tested to balance price and weight reduction. Performance of the fuel cell and its duration were identified using polarisation measurements. A serious novelty of this study is the use of an innovative identification and quantification of performance. The utmost power density of 5.23 mW cm^{-2} was achieved using Titanium as anode current collector and Stainless Steel as cathode current collector at a methanol concentration of 7 M.

The durability tests showed a lifetime about 200 h and a reduction in efficiency of fuel cell by 41% from original value.

Tabbi et al. [6], in their investigation, identified that the automobile industry is encouraging the use of metals as current collector plates as metals having small thickness and weight as well as good conductivity both thermally and electrically. Using stainless steel would reduce the cost, but non-coated SS from investigation still has some challenge with surface-insulating layer of chromium oxide (Cr_2O_3).

Seema et al. [7] has made comprehensive review on recent material development of passive direct methanol fuel cell and emphasis on the performance activity, cost, durability and stability aspects. Each component with their material development along with basic desirable characteristics is reported in this paper. This paper has also reviewed all possible materials of passive DMFC component, which might make the passive DMFC compact and feasible energy source in future.

Mallick et al. [8] in their study on critical review of current collectors for passive direct methanol fuel cells has emphasis on the important aspects such as profile of the current collectors including materials of construction of the current collectors. A number of current collectors of passive DMFC have been selected and reviewed thoroughly. However, very less research works have been found concerning to decrease in the weight of the current collectors as the current collector majorly contributes on the total weight of pDMFC and affects the gravimetric energy density of the fuel cell.

3 Objective

After going through the literature study, it is inferred that the materials of the current collectors influence the performance of the pDMFC. Required properties of the current collector materials are high electrical conductivity at operating zone, thermal conductivity to optimise and to maintain the thermal stability of cell during operation and high corrosion resistance having compatibility in dilute methanol environment. After considering the desirable properties of the bipolar plates, this experimental study has been taken up to identify the better current collector materials combination among Nickel-201, brass and SS-316L current collectors in anode–cathode ends.

4 Problem Description

Current collectors of passive direct methanol fuel cell play as a key component, and the performance of the fuel cell depends on its material of construction, dimensions and novel design with shape factors. The weight of the current collectors contributes almost 3/4 of the total weight of the cell [9]. Hence, the gravitational power density is significantly affected by the selection of current collector materials and its design aspects.

The required characteristics of materials [10] of the current collectors in pDMFC are as follows:

1. Good electrical conductivity or very low electrical resistivity at operating zone of the direct liquid feed methanol cell [11].
2. High thermal conductivity to optimise and to maintain the thermal stability of cell during operation [12].
3. Desirable mechanical properties like high tensile strength and flexural rigidity of materials [13].
4. Better fabrication and machinability processes of materials [14].
5. Corrosion resistance in methanol environment at various concentrations and wide range of operating temperatures [15].
6. Longer durability and life [16].
7. Low density of materials [17].
8. Easily available at cheaper cost [18].
9. Less contact resistance with the diffusion layers [19].
10. Even distributing and transport area of reactants [20].

The functions of the anode and cathode side current collectors are relatively different; however, they have some of the common aspects like uniform spreading of chemical reactants, maintaining cell structure support, disposal of reaction by products and providing the electrical connectivity with adjacent cells in case of stacking of cells. At the anode, current collector allows the passage of transporting methanol solution and carbon dioxide. Further it collects the electric current from MEA, whereas the cathodic end current collector provides transportation of water, collects the current from cathodic end diffusion layer and receives the oxidant from ambient air.

Details of the materials compositions are given in Table 1 [21], and properties of the materials are provided in Table 2.

5 Experimental Set-Up

To evaluate performance of passive DMFC with the combination of Nickel-201, brass and SS-316L current collectors, a single direct methanol fuel cell fixture is selected. For carrying out this experimental testing, different anode and cathode current collector materials, fabricated with 2.00 (± 0.02) mm thickness sheets, are used. The circular openings of 100 numbers, in 10 by 10 matrix pattern, are made using 3.8-mm diameter drill. Fabrication drawing detail of the current collector is shown in Fig. 2.

Nafion-117 solid electrolyte is used as permeable membrane in membrane electrode assembly. The anode catalyst layer (ACL) is made up of Pt-Ru (1:1)/C with a catalyst loading of 4 mgcm⁻², and on cathode catalyst layer (CCL), it is made up of Pt/C with a catalyst loading of 2 mg cm⁻². To prevent methanol solution and oxidant leakages, PTFE sealing gaskets are provided in between current collectors

Table 1 Material composition

Composition, Element	Material (% by weight)		
	Stainless steel-316L	Nickel-201	Brass
Carbon, C	0.03 max	0.02 max	–
Manganese, Mn	2.0 max	0.35 max	–
Silicon, Si	0.75 max	0.35 max	–
Phosphorus, P	0.045 max	–	–
Sulphur, S	0.03 max	0.01 max	–
Chromium, Cr	16–18	–	–
Nickel, Ni	10–14	99.00 min	~ 0.05
Copper, Cu	–	0.25 max	65–70
Zinc, Zn	–	–	35–30
Nitrogen, N	0.1 max	–	–
Iron, Fe	Balance	0.40 max	~ 0.4

Table 2 Properties of materials

Material of construction	Maximum corrosion rate in pure methanol, (mm/year)	Density of material, (kg/m ³)	Electrical resistivity of material at 20°C, (X10 ⁻⁷ Ωm)
SS-316L	0.5	7900	7.4
Ni-201	0.05	8890	0.68
Brass	1.25	8500	0.62

and MEA components of the cell. The fabricated active area of the cell is 5.0 cm × 5.0 cm. Methanol solution with 5 M concentration has been prepared to use in this experiment. The required clamping of the cell assembly is made using M8 fasteners, and uniform tightening of the bolts is ensured using a torque wrench which is pre-set at 5Nm value. The experimental set-up of the DMFC is shown in Fig. 3.

6 Experimental Methodology

To evaluate performance of passive DMFC with the combination of Nickel-201, brass and SS-316L current collectors, four set-ups of anode and cathode combinations as referred in Table 3 with single direct methanol fuel cell fixture are chosen. As brass is getting reacted with dilute methanol with the formation of metal methoxides, the use of brass as current collector material in anode side is not considered. As Ni and SS material are performed better at 5 M, experiments have been carried out at this concentration of methanol solution.

Fig. 2 Fabrication drawing detail of current collector

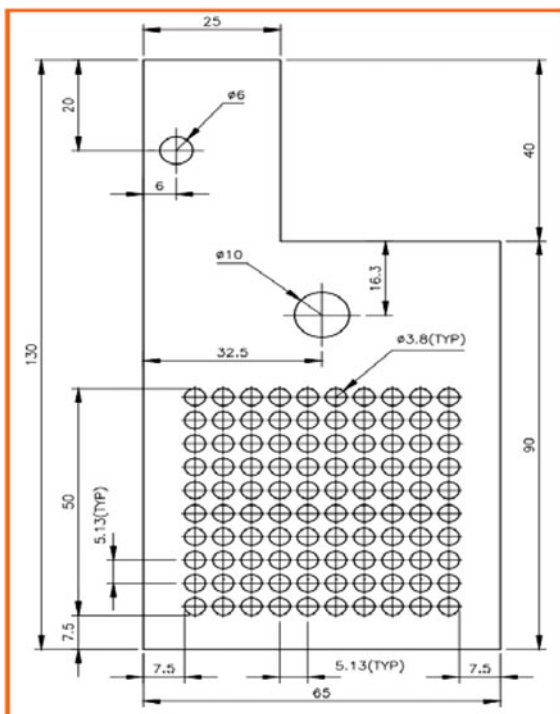


Fig. 3 Experimental set-up of passive DMFC

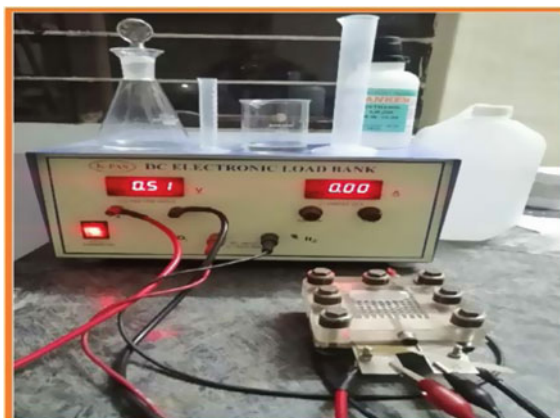


Table 3 Experimental set-up

Set-up	Anode	Cathode
I	Nickel-201	Stainless steel, Gr 316L
II	Nickel-201	Brass (70/30)
III	Stainless steel, Gr 316L	Nickel-201
IV	Stainless steel, Gr 316L	Brass (70/30)

While performing the experiment, the first set of voltage and current readings has been taken by varying current characteristic conditions using Nickel-201/SS-316L (set-up-I) materials as current collectors at 5 M methanol concentration. This experiment further repeated with the other mentioned set-up-II, Nickel-brass; set-III Stainless Steel-Nickel and with set-up-IV Stainless Steel-brass current collectors, and corresponding voltage and current characteristics have been noted. Total experiment has been repeated thrice at this 5 M concentration methanol solution to get repeatability and consistency in the readings. Mean value of the three readings of observations corresponding to current–voltage is taken for analysis of the cell characteristics.

7 Experimental Results and Analysis

7.1 Polarisation and Power Density Characteristics

In the experimental set-up-I, Nickel-201 material as anode and SS316L as cathode current collector have been used. Cell is tested with 5 M methanol solution concentration at ambient conditions. In this experiment, the highest power density recorded is 6.720 mW cm^{-2} at current density of 32.0 mA cm^{-2} . During testing, the maximum current density that recorded is 62.4 mA cm^{-2} at 5 M methanol concentration.

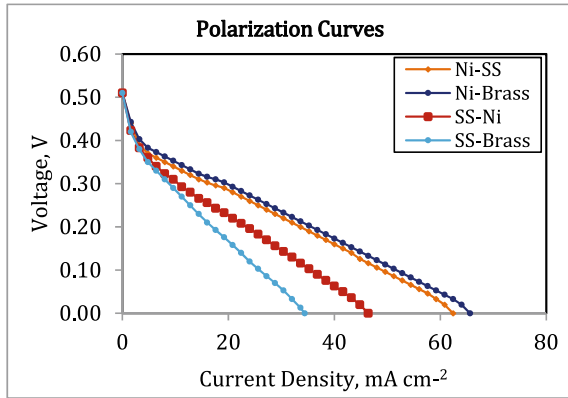
In the experimental set-up-II, Nickel-201 material as anode and brass as cathode current collector have been used. Cell is tested with 5 M methanol solution concentration at ambient conditions. In this experiment, the maximum power density recorded is 7.157 mW cm^{-2} at a current density of 33.6 mA cm^{-2} . During testing, the maximum current density recorded is 65.6 mA cm^{-2} at 5 M methanol concentration.

In the experimental set-up-III, SS316L material as anode and Nickel-201 as cathode current collector have been used. Cell is tested with 5 M methanol solution concentration under ambient conditions. In this experiment, the peak power density recorded is 4.704 mW cm^{-2} at a current density of 24.0 mA cm^{-2} . During testing at the same 5 M methanol concentration, the largest current density recorded is 46.4 mA cm^{-2} .

In the experimental set-up-IV, SS316L material as anode and brass as cathode current collector have been used. Cell is tested with 5 M methanol solution concentration in ambient conditions. In this experiment, the highest power density recorded is 3.397 mW cm^{-2} at a current density of 17.6 mA cm^{-2} . During testing, the maximum current density recorded is 34.4 mA cm^{-2} at 5 M methanol concentration.

Polarisation curves (voltage–current density characteristics) of the four set-ups of pDMFC configuration are plotted as shown in Fig. 4. Initially when current density is zero, the cell generated voltage is maximum (open circuit voltage), and as the current density increases, the cell voltage decreases to zero. From Fig. 4, Nickel-brass combination as anode and cathode is performing better with the highest current density as revealed in polarisation characteristics.

Fig. 4 Voltage–current density characteristics



Power density curves (power density versus current density characteristics) of these four set-ups of pDMFC configuration are plotted as shown in Fig. 5. Power density of the cell increases from zero to a maximum value, and further, it decreases to zero with increase in the current density. Nickel-brass combination as anode and cathode is performing better with maximum power density as revealed from the drawn characteristics.

The combined voltage and power density superimposed characteristics against the current density are plotted as shown in Fig. 6.

Fig. 5 Power density characteristics

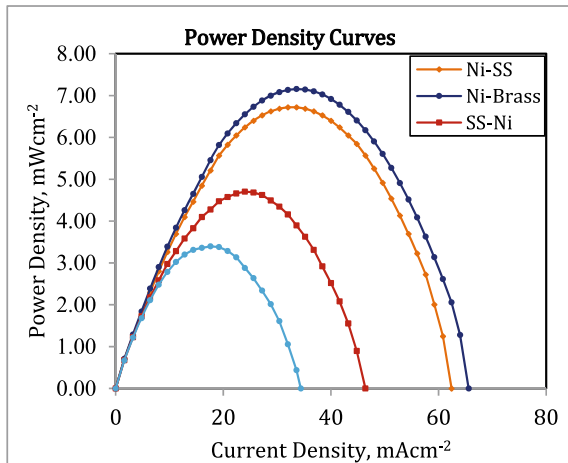
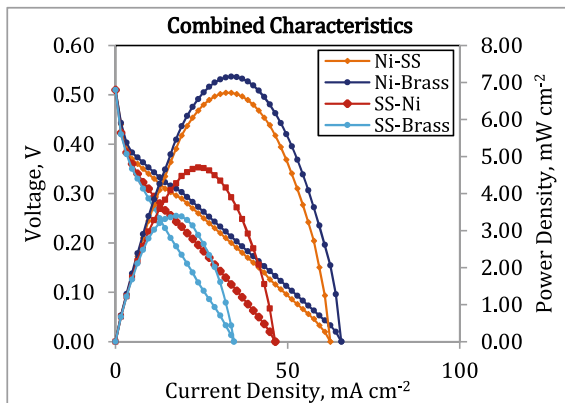


Fig. 6 Voltage and power density superimposed curves



7.2 Comparison of Maximum Power Density and Maximum Current Density

Results of the four set-ups with current collectors against current density and power density are taken for analysis. Bar charts of current collectors' combinations as anode-cathode materials versus maximum power density produced (refer to Fig. 7) and current density (ref to Fig. 8) are drawn. Anode-cathode combination of Nickel-brass showed better current density and power density among these four set-ups, and SS-brass combination showed the least performance. Better performance of Nickel is due to higher conductivity and higher resistance to methanol solution, whereas brass has superior conductivity but lack of compatibility with methanol solution. For short-term applications, Ni-brass combination is satisfactory, but for long-term applications, Ni-SS is better, as Nickel and SS materials have better compatibility in methanol environment compared to brass.

8 Conclusions

In the commercialisation process of the passive direct methanol fuel cell (pDMFC), market demands for efficient systems with optimisation of components performance with respect to durability and effectiveness. The desirable qualities of the current collector materials are excellent electrical conductivity and high thermal conductivity to optimise and to maintain the thermal stability of cell during operation and high corrosion resistance with compatibility in dilute methanol environment. These aspects are experimentally investigated with the combination of anode and cathode current collectors, fabricated with an opening ratio of 45.3% with combination set-ups, set-up-I, Nickel-Stainless steel; set-up-II, Nickel-brass; set-up-III

Fig. 7 Maximum power density versus anode–cathode materials

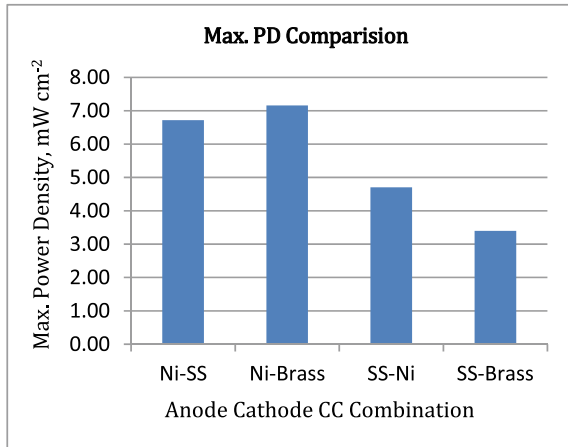
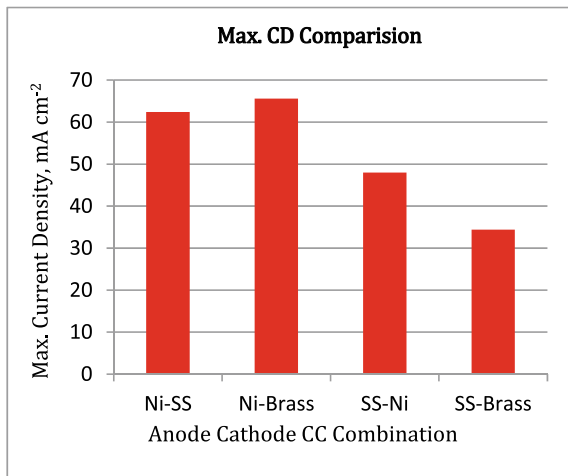


Fig. 8 Maximum current density versus anode–cathode materials



Stainless Steel-Nickel and with set-up-IV Stainless Steel-brass materials. The anode–cathode combination of set-up-II, Nickel-brass showed the best current density (46.4 mA cm⁻²) and power density (7.157 mW cm⁻²), and set-up-IV, SS-brass combination showed the least performance with current density (34.4 mA cm⁻²) and power density (3.397 mW cm⁻²). Superior performance of Nickel is due to good electrical conductivity and better corrosion resistance to dilute methanol solution, whereas brass has the best electrical conductivity among the selected materials but suffers lack of compatibility with methanol solution. For short-term durations, Ni-brass combination performance is found satisfactory, but for long-term applications Ni/SS-316L is better as these materials have excellent compatibility and corrosion resistance in methanol environment compared to brass. In future investigations, materials that are

suitable in dilute methanol environment either bare or with electrical conducting coatings may be used with combination of current collectors.

References

1. O'Hayre R, Cha S-W, Colella W, Prinz FB (2016) Fuel cell fundamentals, 3rd edn. John Wiley & Sons Inc., New Jersey
2. Raghavaiah NV, Naga Srinivasulu G, HariPrasad I (2020) Review of challenges in direct methanol fuel cell and contemporary status. *Res Appl Thermal Eng* 3(2):1–8. <https://doi.org/10.5281/zenodo.3989515>
3. Kamarudin SK, Achmad F, Daud WRW (2009) Overview on the application of direct methanol fuel cell (DMFC) for portable electronic devices. Published by Elsevier Ltd., International Association for Hydrogen Energy. <https://doi.org/10.1016/j.ijhydene.2009.06.013>
4. Boni M, Srinivasa Rao S, Naga Srinivasulu G (2020) Performance evaluation of an air breathing–direct methanol fuel cell with different cathode current collectors with liquid electrolyte layer. *Asia-Pac J Chem Eng* 2020:2465. <https://doi.org/10.1002/apj.2465>
5. Braz BA, Oliveira VB, Pinto AMFR (2020) Optimization of a passive direct methanol fuel cell with different current collector materials. *Energy* 208:118394
6. Wilberforce T, Ijaodola O, Ogungbemi E, El Hassan Z, Thompson J (2018) Effect of bipolar plate materials on performance of fuel cells. Module in Mater Sci Mater Eng. <https://doi.org/10.1016/B978-0-12-803581-8.11272-X>
7. Munjewar SS, Thombre SB, Mallick RK (2017) A comprehensive review on recent material development of passive direct methanol fuel cell, *Ionics* vol 23, pp 1–18
8. Mallick RK, Thombre SB, Shrivastava NK (2015) A critical review of the current collector for passive direct methanol fuel cells. *J Power Sources* 285:510–529
9. Yuan W, Tang Y, Yang X, Liu B, Wan Z (2012) Structural diversity and orientation dependence of a liquid-fed passive air-breathing direct methanol fuel cell. *Int J Hydrogen Energ* 37:9298–9313
10. Raghavaiah NV (2019) Overview of pressure vessel design using ASME boiler and pressure vessel code section viii division-1 and division- 2. *Int J Res Eng Sci Manage* 2(6):525–526
11. YangaW M, ChoubC SK (2007) Shua 2007, Effect of current-collector structure on performance of passive micro direct methanol fuel cell. *J Power Sources* 164(2):549–554. <https://doi.org/10.1016/j.jpowsour.2006.11.014>
12. Dohle H, Mergel J, Stolten D (2002) [2002], Heat and power management of a direct-methanol-fuel-cell (DMFC) system. *J Power Sources* 111(2):268–282
13. Huang J, Baird DG, McGrath JE (2005) Development of fuel cell bipolar plates from graphite filled wet-lay thermoplastic composite materials. *J Power Sources* 150:110–119. <https://doi.org/10.1016/j.jpowsour.2005.02.074>
14. Abraham BG, Chetty R (2021) Design and fabrication of a quick-fit architecture air breathing direct methanol fuel cell. *Int J Hydrogen Energ* 46(9), pp 6845–6856
15. Song SQ, Liang ZX, Zhou WJ, Sun GQ, Xin Q, Stergiopoulos V, Tsiakaras P (2005) Direct methanol fuel cells: The effect of electrode fabrication procedure on MEAs structural properties and cell performance. *J Power Sources* 145(2):495–501. <https://doi.org/10.1016/j.jpowsour.2005.02.069>
16. Cha H-C, Chen C-Y, Shiu J-Y (2009) Investigation on the durability of direct methanol fuel cells. *J Power Sources* 192(2):451–456. <https://doi.org/10.1016/j.jpowsour.2009.03.028>
17. Kuan Y-D, Lee S-M, Sung M-F (2014) Development of a direct methanol fuel cell with lightweight disc type current collectors. *Energies* 7:3136–3147. <https://doi.org/10.3390/en7053136>
18. Sgroi M, Zedde F, Barbera O, Stassi A, Sebastián D, Lufrano F, Schuster M (2016) Cost analysis of direct methanol fuel cell stacks for mass production. *Energies* 9(12):1008. <https://doi.org/10.3390/en9121008>

19. Braz BA, Oliveira VB, Pinto AM (2020) Experimental evaluation of the effect of the anode diffusion layer properties on the performance of a passive direct methanol fuel cell. *Energies*13:5198. <https://doi.org/10.3390/en13195198>
20. Shrivastava NK, Harris TA (2017) Direct methanol fuel cells. *encyclopedia of sustainable technologies*, pp 343–357. <https://doi.org/10.1016/b978-0-12-409548-9.10121-6>
21. Properties of Some Metals and Alloys (2021) Nickel Institute, [https://nickelinstitute.org/media/1771/propertiesofsomemetals and alloys_297_pdf](https://nickelinstitute.org/media/1771/propertiesofsomemetals%20and%20alloys_297.pdf).

Performance Comparison of Different Geometries of Thermal Energy Storage Unit for Solar Cooker



B. C. Anilkumar, Ranjith Maniyeri, and S. Anish

Abstract Many researchers have been interested in solar energy as an unlimited energy resource over the last few decades due to its vast range of applications, including household cooking. The present work aims to design, optimize, fabricate, and test different geometries of thermal energy storage (TES) units for solar cooker (SC) using paraffin wax as the phase change material (PCM). The optimum amount of PCM necessary for different geometries (cylindrical, square, and hexagonal) of TES units surrounding the cooking vessel is computed using a computational approach. The TES units developed in this study have the provisions for filling the PCM on all sides, including the lid, enhancing the heat transfer to the cooking load. The performance comparison of different TES units is carried by conducting the indoor test. The experimental findings show that after 6 h, all geometries of TES units maintain the temperature of the cooking load at the melting point of PCM. However, cylindrical-shaped TES unit performs best in comparison with hexagonal and square. A cylindrical box solar cooker performance test is also carried out with an optimized cooking vessel surrounded by the PCM-filled TES unit and lid.

Keywords Cylindrical box solar cooker · Thermal energy storage unit · Phase change material · Cooking pot

Nomenclature

T_{mp} Melting temperature of PCM
 M_{pcm} Mass of PCM
 U Overall heat transfer coefficient

B. C. Anilkumar · R. Maniyeri (✉) · S. Anish
Department of Mechanical Engineering, National Institute of Technology Karnataka (NITK),
Surathkal, Mangalore, Karnataka 575025, India
e-mail: mranjil@nitk.edu.in

S. Anish
e-mail: anish@nitk.edu.in

Greek Symbol

λ Latent heat of fusion of PCM

1 Introduction

Renewable energy systems, particularly solar cookers (SCs), are viable for meeting global cooking needs. SC converts the insolation into useful thermal energy for cooking. Solar energy has become more prominent in the present worldwide debate on energy and the environment. Today, growing awareness for the benefits of renewable energy and increasing prices of fossil fuels drive the SC market. Many modifications were made to SCs over the last four to five decades across the world [4, 5]. In a recent study, we examined the effects of various box shapes on solar cooker performance by using numerical analysis, including rectangular, trapezoidal, cylindrical, and frustums of cones [3].

The evening or night cooking is possible with the provision of the heat storage facility in SCs. Thermal energy can be stored in the SC as sensible or latent heat. Generally used sensible heat storage materials (SHSMs) in SCs are sand [13], engine oil [10], and carbon [15]. In our recent study [1], we experimentally investigated the effects of the optimum mixture of SHSMs such as sand, iron grits, brick powder, and charcoal on the performance of solar box cooker (SBC). In the latent heat storage (LHS) units, energy stored during a phase change is used for cooking. Generally, phase change materials (PCMs) are used to store heat energy in the latent form. The cooking pot incorporated with the LHS system contains two concentric cylindrical vessels made of aluminium or steel with an annular cavity filled with PCM (Fig. 1). The PCMs contained in the cooking vessel are heated and solidified by the SBC or concentrated/indirect SCs. Recently, several review papers [12, 17] are reported on the developments of SCs incorporated with PCMs. Nkhonjera et al. [11] reviewed the heat storage units, materials, and performance of SCs included with thermal energy storage (TES) units. They recommended that the shape and heat transfer properties of TES units need be optimized.

In general, the TES units surrounding the cooking vessel were filled with PCM along the lateral side [6–9, 16, 18]. In the present work, we aim to introduce a new design of the TES unit that includes the facility for filling the PCM at the bottom part of the cooking pot and on the lid. This will enhance the cooking performance as heat is transferred to the load through all sides of the pot. Therefore, the primary objective of this research is to design and develop the TES units of different geometries incorporated with the cooking pot. The present study also compares the cylindrical, square, and hexagonal geometry of TES units by conducting the indoor test. Another goal of this research is to conduct outdoor tests to evaluate the performance of the improved TES unit with the cylindrical box solar cooker (CBSC). The optimum

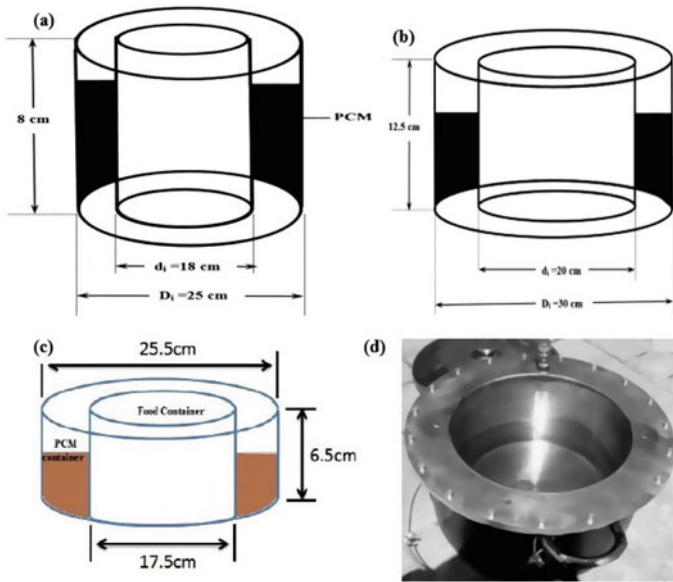


Fig. 1 Schematic of TES units for solar cooker **a** Buddhi et al. [7] **b** Sharma et al. [16] **c** Vigneswaran et al. [18] **d** Photo of TES unit [8]

mass of PCM and dimensions for the different geometries of TES units are found following our recently developed computational procedure [2].

2 Methodology

Latent Heat Storage Medium: Paraffin wax can reach a wide range of temperatures, thus making it a useful heat storage material in several applications. Paraffin wax is considered as good heat storage material because of its fast-charging properties and high latent heat of fusion. Furthermore, they are non-corrosive, compatible with many materials, chemically stable, non-toxic, and do not segregate. In general, the paraffin wax used as PCM is of technical grade. This grade of paraffin wax is also cost effective, feasible, and widely used. However, they also present some disadvantages, such as low thermal conductivity, more significant volume changes between the solid and liquid phases, and the possibility of flammability.

The solid–liquid phase transition temperature should be around 100 °C or higher for practical cooking. Paraffin wax is available in different fusion temperatures. The melting temperature and latent heat of fusion of paraffin wax tested in SCs by Saxena et al. [14], Yuksel et al. [19], and Lecuona et al. [8] are, respectively, 41–44 °C, 58–60 °C, 100 °C and 250 kJ/kg, 189 kJ/kg, and 140 kJ/kg. Paraffin wax shows a decrease

Table 1 Thermo-physical parameters of commercial-grade paraffin wax

Properties		
Melting temperature (°C)		55–60
Latent heat of fusion (kJ/kg)		220
Density (kg/m ³)	Solid	818
	Liquid	760
Specific heat (kJ/kg °C)	Solid	2.95
	Liquid	2.51
Thermal conductivity (W/m°C)		Liquid 0.22

in latent heat of fusion with increasing melting temperature. In the present work, we used paraffin wax with fusion temperature of 55–60 °C and latent heat of 220 kJ/kg.

Design of TES Unit: The TES units of cylindrical, hexagonal, and square geometries are designed using the previously developed computational procedure [Anilkumar et al. 2021]. The dimension of the TES container depends on the properties of the heat storage material to be used, and the time for the evening or night cooking is required. The thermo-physical parameters of commercial-grade paraffin wax, which is employed as the PCM for heat storage in all geometries, are given in Table 1. For maintaining the temperature of the cooking vessel at PCM's melting point for a specific duration of time, latent heat rejected by the PCM and energy loss from the container should be equal. This is expressed by the equation [13]

$$M_{pcm}\lambda = U(T_{mp} - T_a)t \quad (1)$$

The procedure to be followed in the design of TES unit is as follows: [3]

Step 1: Initially guess the temperatures of PCM, the inner and outer surface of the TES unit, and ambient air.

Step 2: Compute air and PCM's thermal properties (Pr , k , and ν) at the corresponding mean temperature.

Step 3: Calculate the Nusselt number and convective heat transfer coefficient at the inner and outer surface of the TES unit using analytical correlations.

Step 4: Guess the dimension of the TES unit of each geometry.

Step 5: Compute U-value for each geometry of the heat storage container.

Step 6: Compute the mass of PCM required using Eq. (1).

Step 7: Update the dimension of the TES unit.

Step 8: Compare the updated and previous dimension value and repeat the step 5 to 7 until it converges.

Step 9: Update the temperature at the inner and outer surfaces of the TES unit.

Step 10: Compare the updated and previous temperature values and repeat the step 2 to 9 until it converges.

The mass of paraffin wax required and dimensions of heat storage containers of different geometries surrounding the cooking vessel of diameter 16 cm and height

Table 2 Dimensions of different geometries of TES units and required mass of PCM

Geometry	Dimension of TES container (cm)	Mass of PCM (kg)		
		Lateral side	Bottom side + Lid	Total
Cylindrical	18.7	1.01	0.416	1.426
Hexagonal	10.7	1.32	0.452	1.772
Square	17.5	1.44	0.464	1.904

18 cm are given in Table 2. The optimum mass of PCM required for 6 h is found to be maximum for square followed by hexagonal and minimum for the cylindrical geometry. Therefore, a cylindrical-shaped TES unit is considered the optimum geometry as it uses the minimum mass of PCM for maintaining a constant temperature for a specific duration of time.

Fabrication of TES Unit: The TES units of cylindrical, hexagonal, and square geometries (Fig. 2) are fabricated using a stainless steel sheet of 1 mm thickness. The sheet is cut into the required shapes and dimensions by using the automatic CNC machine. Bending and rolling works are carried out using hydraulic press brake bending and rolling machines, respectively. Then the parts are joined by spot/resistance welding at different locations to form the required geometry. Afterwards, the joints are entirely welded by the tungsten inert gas (TIG) welding process. Finally, the grinding process is carried out for the smooth and consistent appearance of the welded parts. Two holes are drilled on the vertical surface of the container facing in the opposite direction for inserting PCM into the cavity. The PCM can be filled in the annular cavity between the inner pot and outer TES container on the lateral side and at the bottom. The lid for all the geometries of TES units is fabricated with provisions for filling the PCM. For this, two holes are provided at the top of the lid in opposite directions.

The designed quantity of PCM should be filled into the TES unit to expand and solidify completely in each cycle. The TES unit is first kept vertically and partially placed in hot water during PCM filling. PCM is filled through one of the provisions at the top. At the same time, the other provision on the opposite side was kept open for the escape of air during filling. After filling at the hole level, one of them is closed, and the container is kept in a horizontal position. Then the PCM is filled, and another provision is also closed. The lid is also filled with PCM by following the same procedure. During the complete filling procedure, PCM is maintained in the liquid state by keeping the TES unit in a hot water bath.

Performance Test: The performance comparison of different geometries of TES units is carried by conducting indoor and outdoor experiments. The indoor test is performed to validate the computational approach used to design the TES containers of all geometries, whereas the outdoor experiment is performed by testing the optimized TES container charged with CBSC.

Indoor test. The experimental set-up for the indoor test is shown in Fig. 3. The temperature of cooking pot surfaces and water is measured by using the K-type

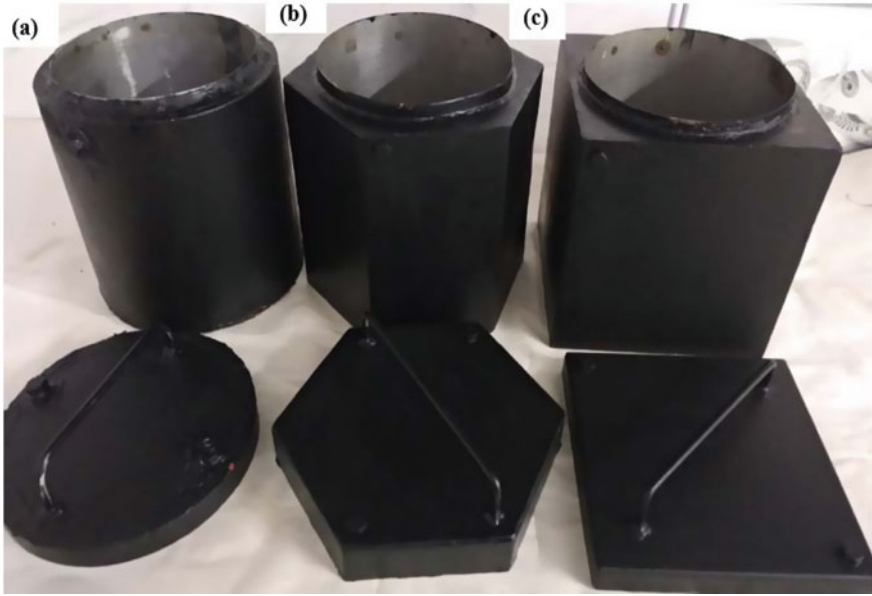


Fig. 2 Cooking pot with TES unit and lid of different geometry **a** cylindrical, **b** hexagonal, and **c** square

thermocouple and an indicator. The container is tested with water for the performance study. Initially, water is heated up to 100 °C and is poured into the vessel fully. Again, water in the vessel is replaced with newly boiled water. Before changing the water, the temperature of the previous water in the container is measured. Also, the temperatures of all the surfaces of the vessel are measured. This process is continued until all the surface temperature reaches the melting temperature of PCM and remains constant after that. This ensures that all PCMs in the container are melted. After PCM gets melted fully, water in the vessel is made empty, and again water at a temperature above the melting point of PCM is filled in the vessel and the lid is closed. The temperature at each surface of the vessel is measured in equal intervals of time. After six hours, the water temperature in the pot is measured and compared with the expected value.

Outdoor test. The performance test of the TES unit with optimum geometry is conducted by charging with CSBC (Fig. 4). The CSBC used in the present work consists of a mild steel cylindrical box with external and internal diameters 53 cm and 43 cm, respectively, and height 30 cm. A double glazed cover is provided at the top of the cooker to form the greenhouse effect, allowing solar radiation to pass into the cavity but preventing it from escaping. Since the glazing is opaque to longer wavelength radiation such as infrared waves emitted by the absorber plate, heat radiation will be trapped inside the cooker. The annular gap between the outer and inner cylinders is insulated with 5-cm-thick glass wool to reduce heat loss to the environment. The circular absorber plate made up of aluminium having a diameter